Ceramics International 44 (2018) 22856–22864

Contents lists available at ScienceDirect

Ceramics International

journal homepage: www.elsevier.com/locate/ceramint

Peculiarities of the dielectric properties of ternary $0.5(Y_{0.1}Zr_{0.9}O_2) - 0.5(0.6SrTiO_3 - 0.4BiScO_3)$ ceramic system

Oleg Ivanov[a,*], Elena Danshina[b]

[a] Belgorod State University, Belgorod 394015, Russian Federation
[b] Belgorod State Technological University named after V.G. Shukhov, Belgorod 308012, Russian Federation

ARTICLE INFO

Keywords:
Ternary ceramic system
Two-component ceramic system
$Y_{0.1}Zr_{0.9}O_2$ and $0.6SrTiO_3 - 0.4BiScO_3$ subsystems
Diffuse phase transition
Dielectric relaxation process

ABSTRACT

Ceramic samples of ternary $0.5(Y_{0.1}Zr_{0.9}O_2) - 0.5(0.6SrTiO_3 - 0.4BiScO_3)$ system consisting of individual $Y_{0.1}Zr_{0.9}O_2$ and $0.6SrTiO_3 - 0.4BiScO_3$ subsystems were synthesized via solid-state processing techniques. By XRD analysis, a coexistence of tetragonal *P42/nmc* phase related to the $Y_{0.1}Zr_{0.9}O_2$ subsystem, and cubic $Pm\bar{3}m$ and tetragonal *P4mm* phases associated with the $0.6SrTiO_3 - 0.4BiScO_3$ subsystem was found. A deviation of real composition from nominal one for both $Y_{0.1}Zr_{0.9}O_2$ and $SrTiO_3 - BiScO_3$ subsystems due to Sc substituting for Zr in the $Y_{0.1}Zr_{0.9}O_2$ subsystem and, vice versa, Zr substituting for Sc in the $SrTiO_3 - BiScO_3$ subsystem was also observed. Peculiarities of the dielectric properties related to both diffuse ferroelectric phase transition and dielectric relaxation processes were found and analyzed in comparison with the dielectric properties of two-component $0.6SrTiO_3 - 0.4BiScO_3$ system. It was found that the diffuse phase transition in ternary system, firstly, shifts to lower temperatures and, secondly, has a less degree of diffuseness as compared to two-component system. Such kind of behavior could be attributed to a difference of ionic radii of ions Zr^{4+} and Sc^{3+}. Dielectric relaxation processes associated with the O^{2-} ions migration were observed within temperature 500–800 K for both ternary and two-component systems. Two dielectric relaxation processes related to the $Y_{0.1}Zr_{0.9}O_2$ and $0.6SrTiO_3 - 0.4BiScO_3$ subsystems were found in ternary system, whereas one dielectric relaxation process was observed in two-component system. The activation energies for the dielectric relaxation processes were estimated as ~ 1.3 eV and ~ 0.9 eV for $Y_{0.1}Zr_{0.9}O_2$ and $0.6SrTiO_3 - 0.4BiScO_3$ subsystems, respectively, for ternary system, and ~ 0.75 eV for two-component system.

1. Introduction

Ternary $0.5(Y_{0.1}Zr_{0.9}O_2) - 0.5(0.6SrTiO_3 - 0.4BiScO_3)$ system should be considered as consisting of two individual subsystems. The first subsystem is zirconium dioxide, ZrO_2, stabilized by Y, so that nominal composition of this subsystem is corresponding to $Y_{0.1}Zr_{0.9}O_2$. The second subsystem is two-component $SrTiO_3 - BiScO_3$ system with a ratio of end members corresponding to the $0.6SrTiO_3 - 0.4BiScO_3$ composition. Ternary $0.5(Y_{0.1}Zr_{0.9}O_2) - 0.5(0.6SrTiO_3 - 0.4BiScO_3)$ system is attractive to be studied in details due to both interesting properties of the individual subsystems and a change in these properties via a combination of the subsystems in a single system.

For instance, yttria stabilized zirconium dioxide, $Y_xZr_{1-x}O_2$, possessing a high ionic conductivity is conventional material using as solid electrolyte for solid oxide fuel cells [1–3]. In turn, a high mechanical strength of ZrO_2 is very attractive advantage for various structural applications [4,5]. Strontium titanate, $SrTiO_3$, is known to be an incipient ferroelectric lying near limit of its paraelectric phase stability [6]. Pure $SrTiO_3$ retains a nonpolar centrosymmetric structure upon cooling at $T \rightarrow 0$ K. But, various ions substituting for host ions in *A*- or/and *B*-positions in the perovskite ABO_3 structure can induce a ferroelectric phase transition in $SrTiO_3$ [7–12]. $BiScO_3$ is interesting end member for fabrication of new ceramic solid solutions [13–15]. Despite its utility in the solid solutions, there is little knowledge about the $BiScO_3$ member itself. In particular, it is not known at present whether $BiScO_3$ is ferroelectric [16]. Thus, pure $SrTiO_3$ and $BiScO_3$ can be considered as nonferroelectric compounds. However, the $SrTiO_3$-$BiScO_3$ system consisting of nonferroelectric end members is already characterized by dielectric anomalies specific for relaxor ferroelectrics (or ferroelectrics with a diffuse phase transition) [17,18]. The main features of relaxors are related to their structural (compositional) inhomogeneity [19–21]. In terms of structural features, the relaxor properties can be attributed to coexistence and interaction of polar and nonpolar phases within a temperature range, where the relaxor state

* Corresponding author.
E-mail address: Ivanov.Oleg@bsu.edu.ru (O. Ivanov).

https://doi.org/10.1016/j.ceramint.2018.09.078
Received 18 July 2018; Received in revised form 22 August 2018; Accepted 8 September 2018
Available online 10 September 2018

exists.

Based on analysis of literature data, a few scientific and technics tasks requiring various combinations of ZrO_2 and $SrTiO_3$ should be mentioned. Firstly, glass-ZrO_2-$SrTiO_3$ mixture with a controlled temperature coefficient of the dielectric permittivity was developed in Ref. [22]. In this mixture, $SrTiO_3$ is responsible for the dielectric properties, whereas ZrO_2 has to maintain the mechanical strength. Secondly, ultrathin film heterostructures based on the ZrO_2-$SrTiO_3$ system are among prospective systems having a great potential for applications as solid electrolyte materials [23–25]. These heterostructures contain nanosized interfaces between the individual ZrO_2 and $SrTiO_3$ layers. In turn, such kind of interfaces have a specific atomic arrangement favouring the effective transport of oxygen ions under external electric field within a wide temperature range.

Instead of pure $SrTiO_3$, two-component $SrTiO_3$-$BiScO_3$ subsystem could reasonably be used to modify the properties of the ZrO_2-$SrTiO_3$ system. The matter is that both dielectric properties and ionic transport in solids are strongly dependent on their structural disorder and compositional inhomogeneity [19,23,26]. The structural disorder in $SrTiO_3$ with the perovskite ABO_3 structure can easily be created by substitution on the *A*- and the *B*-sites by ions having ionic radii different from radii of the host Sr^{4+} and Ti^{2+} ions. The *A*- and *B*-sites ion substitution can be implemented at a fabrication of two-component systems by using $SrTiO_3$ as one of end members. Two-component $SrTiO_3$-$BiScO_3$ system can be taken as an excellent example of such kind of systems where the structural disorder degree increases with increasing mole fraction of $BiScO_3$ [17,18].

During the preparation of materials based on ternary $0.5(Y_{0.1}Zr_{0.9}O_2)$ – $0.5(0.6SrTiO_3$ – $0.4BiScO_3)$ system, an interaction between the separate subsystems can take place resulting in deviation of real chemical composition of the subsystems from nominal one and, hence, in changes of their both microstructure and properties. The dielectric properties of solids are sensitive to a change of their microstructure and composition. So, the aim of present work is to find and analyze the peculiarities of the dielectric properties of ternary ceramic $0.5(Y_{0.1}Zr_{0.9}O_2)$ – $0.5(0.6SrTiO_3$ – $0.4BiScO_3)$ system, in which interaction between the individual $Y_{0.1}Zr_{0.9}O_2$ and $SrTiO_3$ – $BiScO_3$ subsystems is expected. To underline the peculiarities characteristic for ternary $0.5(Y_{0.1}Zr_{0.9}O_2)$ – $0.5(0.6SrTiO_3$ – $0.4BiScO_3)$ system, the dielectric properties of this system will be compared to that of two-component $0.6SrTiO_3$ – $0.4BiScO_3$ system.

2. Materials and methods

Ceramic $0.5(Y_{0.1}Zr_{0.9}O_2)$ – 0.5 $(0.6SrTiO_3$ – $0.4BiScO_3)$ samples were synthesized using solid-state processing techniques.

To prepare the $0.6SrTiO_3$ – $0.4BiScO_3$ subsystem, $SrTiO_3$ was at first prepared by sintering an equimolar mixture of the $SrCO_3$ and TiO_2 powders at 1623 K for 2 h. Then, a mixture of the $SrTiO_3$, Bi_2O_3 and Sc_2O_3 powders taken in stoichiometric ratio was calcined at 1523 K for 2 h. Finally, a mixture of the $Y_{0.1}Zr_{0.9}O_2$ and $0.6SrTiO_3$ – $0.4BiScO_3$ powders was cold isostatically pressed at 75 MPa and then calcined at 1543 K for 3 h. To stabilize the tetragonal ZrO_2 structure, 10 at% Y_2O_3 additive was used. All of heat treatments applied to prepare material being studied were carried out in air atmosphere.

X-ray diffraction (XRD) analysis was performed using a Rigaku Ultima IV diffractometer with CuK_α radiation to determine the phase composition and the crystal structure of the samples prepared.

To examine microstructure peculiarities of the samples, a Quanta 200 3D scanning electron microscope (SEM) was applied. Energy dispersive X-ray spectroscopy (EDX) method was also used to determine a content of various chemical elements.

The real, ε', and imaginary, ε'', parts of the complex dielectric permittivity of the samples with Ag electrodes were measured at various measuring frequencies, ν, by using a Novocontrol Concept 43 impedance meter above room temperature or a BR2876 LRC-meter below room temperature.

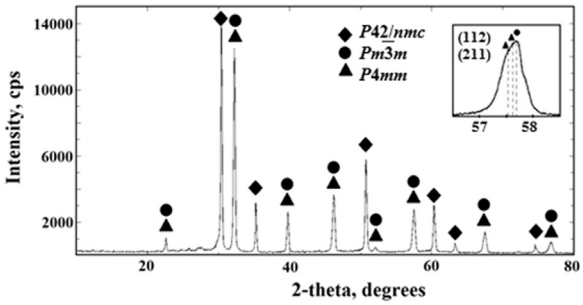

Fig. 1. The XRD pattern of the $0.5(Y_{0.1}Zr_{0.9}O_2)$ – $0.5(0.6SrTiO_3$ – $0.4BiScO_3)$ ceramics. The indexing is based on one cubic $Pm\bar{3}m$ and two tetragonal *P42/nmc* and *P4mm* unit cells. Inset is superposition of three XRD peaks for the tetragonal *P4mm* and cubic $Pm\bar{3}m$ unit cells.

3. Results and discussion

3.1. Crystal and grain structure, phase and elemental composition

According to the XRD pattern taken at room temperature, the ceramic samples with nominal $0.5(Y_{0.1}Zr_{0.9}O_2)$ – $0.5(0.6SrTiO_3$ – $0.4BiScO_3)$ composition consist of three phases (Fig. 1). One phase corresponding to the tetragonal *P42/nmc* structure is characteristic for the $Y_{0.1}Zr_{0.9}O_2$ subsystem. Two other phases with the cubic $Pm\bar{3}m$ and tetragonal *P4mm* structures should be attributed to the $SrTiO_3$ – $BiScO_3$ subsystem [17,18,27].

Actually, the crystal symmetries of end members in the $SrTiO_3$-$BiScO_3$ subsystem are remarkably different. At room temperature, $SrTiO_3$ has the perovskite cubic *Pm3m* structure [7], while $BiScO_3$ is the perovskite-like monoclinic *C2/c* compound [28]. Moreover, a difference in radii for pairs of ions located at equivalent sites in the crystal structure is big. Indeed, taking into coordination numbers characteristic for the perovskite ABO_3 lattice, these radii for $SrTiO_3$ are equal to $r(Sr^{2+}) = 1.44$ Å and $r(Ti^{4+}) = 0.605$ Å. In turn, $r(Sc^{3+}) = 0.745$ Å and $r(Bi^{3+}) = 1.03$ Å are ionic radii for $BiScO_3$. So, taking into account a big enough difference in both crystal symmetries and ionic radii, some intermediate phases with the symmetries other than the cubic $SrTiO_3$ and monoclinic $BiScO_3$ symmetries could be formed to ensure a significant change in the crystal structure of the $(1\text{-}x)SrTiO_3$-$xBiScO_3$ compounds, when the mole $BiScO_3$ fraction, x, increases. Indeed, a coexistence of the tetragonal *P4mm* and cubic *Pm3m* phases within some temperature range dependent on composition was earlier found for the ceramic $(1\text{-}x)SrTiO_3$-$xBiScO_3$ samples with $0.0 < x < 0.6$ [17,18,27]. This phase coexistence is originated from a diffuse ferroelectric phase transition of relaxor type.

The diffraction peaks characterizing the cubic and tetragonal phases in the $SrTiO_3$ – $BiScO_3$ subsystem are very close each to other. To distinguish these structures, a splitting of some diffraction peaks occurring in the tetragonal *P4mm* phase should be taken into account. For instance, the tetragonal structure is characterized by splitting of single cubic (211) peak into double diffraction (211)/(112) peaks as shown in the inset to Fig. 1. So, in accordance with composition, three phases characteristic for the $Y_{0.1}Zr_{0.9}O_2$ and $0.6SrTiO_3$ – $0.4BiScO_3$ subsystems have been observed in the ternary $0.5Y_{0.1}Zr_{0.9}O_2$ – $0.5(0.6SrTiO_3$ – $0.4BiScO_3)$ system.

Next to analyze the XRD pattern, the Savitzky-Golay [29] and Sonneveld-Visser [30] methods were applied. By these methods, unit cell parameters of all three phases were extracted. The $a = 5.107$ Å and $c = 5.158$ Å parameters were found for the tetragonal $Y_{0.1}Zr_{0.9}O_2$ phase. These values are in good agreement with literature data [31]. The parameters for the cubic, a_c, and tetragonal, a_t and c_t, phases of the $SrTiO_3$ – $BiScO_3$ subsystem are listed in Table 1. The same parameters, but taken for two-component ceramic $0.6SrTiO_3$ – $0.4BiScO_3$ system

Table 1
Unit cell parameters and tetragonal distortion degree for ternary $0.5(Y_{0.1}Zr_{0.9}O_2) – 0.5(0.6SrTiO_3 – 0.4BiScO_3)$ and two-component $0.6SrTiO_3 – 0.4BiScO_3$ systems.

Composition	a_c, Å	a_t, Å	c_t, Å	η, %
$0.5(Y_{0.1}Zr_{0.9}O_2) – 0.5(0.6SrTiO_3 – 0.4BiScO_3)$	3.922	3.925	3.937	0.3
$0.6SrTiO_3 – 0.4BiScO_3$	3.937	3.932	3.948	0.4

[17,18], is also presented in this Table. The unit cell parameters for the cubic and tetragonal phases of ternary $0.5(Y_{0.1}Zr_{0.9}O_2) – 0.5(0.6SrTiO_3 – 0.4BiScO_3)$ system happened to be a bit less as compared to two-component $0.6SrTiO_3 – 0.4BiScO_3$ system.

It is important to note that the difference in the a_t and c_t parameters results in a change of tetragonal distortion degree expressed as $\eta = (c_t - a_t)/c_t$ from ~0.4 for $0.6SrTiO_3 – 0.4BiScO_3$ down to ~0.3 for $0.5(Y_{0.1}Zr_{0.9}O_2) – 0.5(0.6SrTiO_3 – 0.4BiScO_3)$. In other words, the $SrTiO_3 – BiScO_3$ subsystem in ternary $0.5(Y_{0.1}Zr_{0.9}O_2) – 0.5(0.6SrTiO_3 – 0.4BiScO_3)$ system is tetragonally distorted less than itself two-component $0.6SrTiO_3 – 0.4BiScO_3$ system. This peculiarity can be related to composition variations of the $SrTiO_3 – BiScO_3$ subsystem in ternary $0.5(Y_{0.1}Zr_{0.9}O_2) – 0.5(0.6SrTiO_3 – 0.4BiScO_3)$ system due to the $Y_{0.1}Zr_{0.9}O_2$ subsystem presence.

Two various individual subsystems can also be seen by the SEM experiments (Fig. 2). Two types of the grains can be observed in the SEM image. The first type grains have a rounded shape (the grain *1* in Fig. 2), whereas the second type grains have a clear crystal faceting (the grain *2*). A size of both types grains is almost the same.

To determine an average size of the grains including the grains of both types, the histogram of grain size distribution was plotted (Fig. 3). This histogram can be described by a lognormal unimodal distribution. The lognormal probability density function can be expressed as [32]

$$P(D) = \frac{1}{\sqrt{2\pi}\sigma D} \exp\left(-\frac{(\ln D - \ln \bar{D})^2}{2\sigma^2}\right), \quad (1)$$

where D is the grain size, $\bar{D}$ is the average grain size and σ is the standard deviation of the logarithms of the grain sizes.

The standard deviation is measure of the width of the distribution. By fitting this distribution, the values of $\bar{D}$ and σ were estimated as ~ 2.45 μm and ~ 0.35, respectively.

The EDX method was applied to determine the content of various elements in the grains of both types. The elemental compositions of the

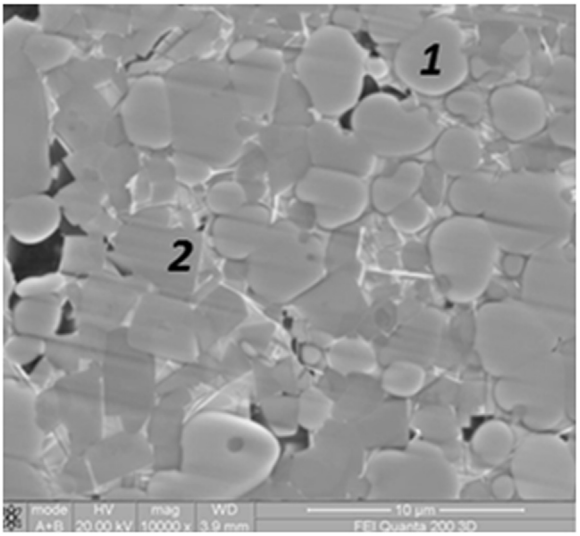

Fig. 2. The SEM image of the $0.5(Y_{0.1}Zr_{0.9}O_2) – 0.5(0.6SrTiO_3 – 0.4BiScO_3)$ surface.

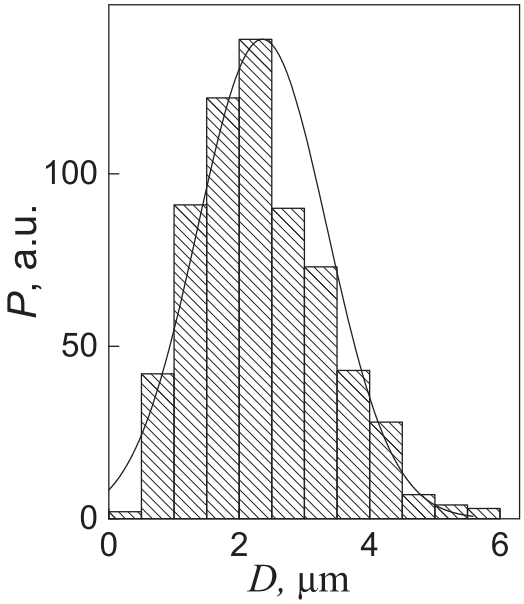

Fig. 3. The histogram of the grain size distribution for the $0.5(Y_{0.1}Zr_{0.9}O_2) – 0.5(0.6SrTiO_3 – 0.4BiScO_3)$ ceramics. Solid line is the fitting curve corresponding to the lognormal unimodal distribution.

Table 2
Elemental composition of various grains in ternary $0.5(Y_{0.1}Zr_{0.9}O_2) – 0.5(0.6SrTiO_3 – 0.4BiScO_3)$ system.

Grain type	Zr, at%	Y, at%	Sr, at%	Ti, at%	Bi, at%	Sc, at%
1	4.29	–	12.26	12.02	7.72	3.69
2	23.32	2.92	–	–	–	6.80

grains *1* and *2* are collected in Table 2. Only cations content was taken into account. First of all, analysis of these data allowed us to conclude that the rounded grains (the grain *1*) correspond to the $SrTiO_3 – BiScO_3$ subsystem, whereas the grains with the crystal faceting (the grain *2*) present the $Y_{0.1}Zr_{0.9}O_2$ subsystem. Besides, a chemical interaction between these subsystems during a high-temperature synthesis results in a change of their nominal chemical composition. Particularly, the $SrTiO_3 – BiScO_3$ subsystem contains Zr, whereas Sc can be found in the $Y_{0.1}Zr_{0.9}O_2$ subsystem. The elemental compositions of the grains *1* and *2* (Table 2) allowed correcting the chemical composition of these grains as $Sr_{0.613}Ti_{0.601}O_{1.8} – Bi_{0.386}Sc_{0.185}Zr_{0.214}O_{1.8}$ instead of $Sr_{0.6}Ti_{0.6}O_{1.8} – Bi_{0.4}Sc_{0.4}O_{1.8}$ (the grain *1*), and $Y_{0.088}Zr_{0.706}Sc_{0.206}O_2$ instead of $Y_{0.1}Zr_{0.9}O_2$ (the grain *2*).

According to Table 2, a deviation of the real composition from nominal one for the $Y_{0.1}Zr_{0.9}O_2$ and $SrTiO_3 – BiScO_3$ subsystems is mainly due to Sc substituting for Zr in the $Y_{0.1}Zr_{0.9}O_2$ subsystem and, vice versa, Zr substituting for Sc in the $SrTiO_3 – BiScO_3$ subsystem. This Sc ↔ Zr substitution is rather expected, since the ionic radius of Sc^{3+} is very close to that of Zr^{4+} (0.745 Å versus 0.720 Å). Moreover, the Zr^{4+} radius is a bit less as compared to that of Sc^{3+}. In this case, the unit cell parameters of the cubic and tetragonal phases in ternary $0.5(Y_{0.1}Zr_{0.9}O_2) – 0.5(0.6SrTiO_3 – 0.4BiScO_3)$ system will also be a bit less as compared to two-component $0.6SrTiO_3 – 0.4BiScO_3$ system in accordance with experimental findings (Table 1). This decrease in the unit cell parameters is naturally accompanied by a decrease in the tetragonal distortion degree.

Since Zr^{4+} and Sc^{3+} have different valence, an electrical neutrality of Zr- or Sc-substituted subsystems will be violated. There are a few mechanisms to recovery the neutrality. For solids based on metal oxides, typical mechanism is due to forming oxygen vacancies. Each oxygen vacancy has a negative charge provided by two electrons. Then,

to compensate extra positive charge of the $SrTiO_3$ – $BiScO_3$ subsystem, where Zr^{4+} partially substitutes for Sc^{3+}, a number of oxygen vacancies have to increase. In turn, an appearance of extra negative charge in the $Y_{0.1}Zr_{0.9}O_2$ subsystem due to Sc^{3+}partially substituting for Zr^{4+} requires decreasing a number of oxygen vacancies. Unfortunately, the oxygen content in the samples studied could not be determined correctly enough to trace any changes in the oxygen subsystem due to recovering the electrical neutrality.

3.2. Peculiarities of dielectric properties due to diffuse phase transition

Now, let us consider the dielectric behavior peculiarities of ternary $0.5(Y_{0.1}Zr_{0.9}O_2)$ – $0.5(0.6SrTiO_3$ – $0.4BiScO_3)$ and two-component $0.6SrTiO_3$ – $0.4BiScO_3$ systems appearing within broad temperature range from ~120 up to ~1000 K. There is two type of the $\varepsilon'(T)$ and $\varepsilon''(T)$ anomalies of various nature.

The first of these dielectric anomalies are the $\varepsilon'(T)$ and $\varepsilon''(T)$ changes characteristic for relaxor ferroelectrics and resulted from a diffuse ferroelectric phase transition occurring in the $SrTiO_3$ – $BiScO_3$ subsystem at low temperatures. The $\varepsilon'(T)$ and $\varepsilon''(T)$ dependences for the $0.5(Y_{0.1}Zr_{0.9}O_2)$ - $(0.6SrTiO_3$ – $0.4BiScO_3)$ and $0.6SrTiO_3$ – $0.4BiScO_3$ systems measured at frequency ν = 1 kHz are presented in Fig. 4. Broad $\varepsilon'(T)$ maxima centered at some temperature T_m observed in these dependences are characterictic for relaxor ferroelectrics [19,33,34]. The T_m value for the $0.5(Y_{0.1}Zr_{0.9}O_2)$ - $(0.6SrTiO_3$ – $0.4BiScO_3)$ system is remarkably lower as compared to that for the $0.6SrTiO_3$ – $0.4BiScO_3$ system. Below T_m, the $\varepsilon''(T)$ dependences for both materials studied start to gradually rise.

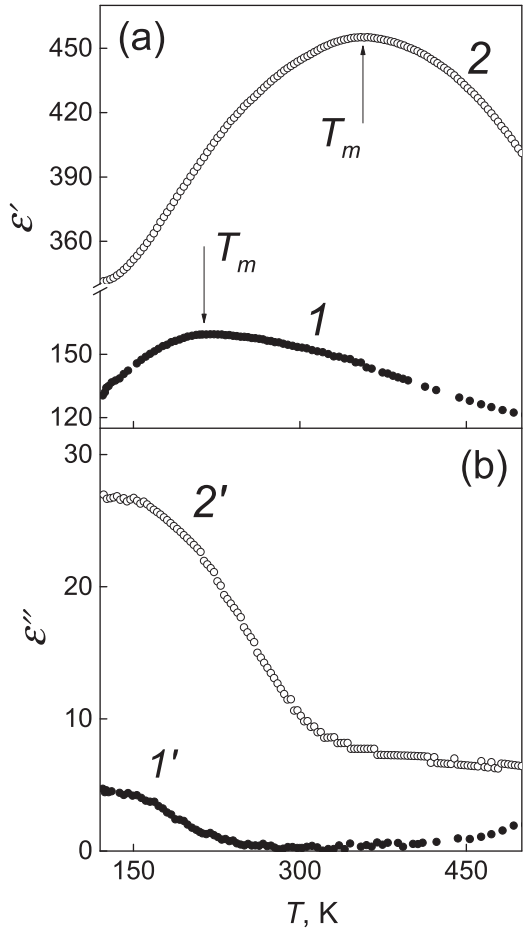

Fig. 4. The temperature ε' (a) and ε'' (b) dependences for the $0.5(Y_{0.1}Zr_{0.9}O_2)$ - $(0.6SrTiO_3$ – $0.4BiScO_3)$ (curves *1* and *1′*) and $0.6SrTiO_3$ – $0.4BiScO_3$ (*2* and *2′*) systems for the diffuse phase transition.

It should be noted that in contrast to conventional ferroelectrics, in relaxor ferroelectrics the temperature T_m does not correspond to the temperature of the phase transition from a paraelectric to a long-range-ordered ferroelectric phase. The polarization in relaxor ferroelectrics is correlated on a local state resulting in appearance of polar nanodomains (PNDs). In this case, the relaxor behavior is related to both appearance and temperature evolution of a polar phase distributed as numerous PNDs inside a nonpolar matrix. The evolution of the relaxor dynamics can be described by using three characteristic temperatures, T_B, T^* and T_f [34].

The temperature T_B called as the Burns temperature indicates an onset of "correlated" polarization fluctuations corresponding to PNDs appearance. These fluctuations are not yet associated with a local strain field and still preserve the local time-averaged nonpolar symmetry characteristic for the high-temperature paraelectric phase. The temperature T_B can be extracted from the temperature dependences of the refractive index or thermal expansion coefficient.

The temperature T^* is positioned lower than the Burns temperature. It corresponds to the temperature at which the relaxor behavior sets in. Below the temperature T_B, the local strain field will eventually develop to stabilize at T^* the PNRs into permanently distorted PNDs having symmetry of the low-temperature ferroelectric phase. The temperature T^* can easily be estimated from the temperature dependence of the dielectric permittivity. Finally, the temperature T_f is the freezing temperature which corresponds to slowing-down of the relaxation related to the reorientation of PNDs. The freezing processes of PNDs are characterized by an anomalously wide spectrum of dielectric relaxation times described by the Vogel-Fulcher dynamics.

Analysis of the experimental $\varepsilon'(T)$ curves in frames of the Curie-Weiss law allowed extracting the T^* values for the $0.5(Y_{0.1}Zr_{0.9}O_2)$ – $0.5(0.6SrTiO_3$ – $0.4BiScO_3)$ and $0.6SrTiO_3$ – $0.4BiScO_3$ systems. As known, for ferroelectrics with a sharp phase transition, the $\varepsilon'(T)$ dependence for high-temperature side of the $\varepsilon'(T)$ peak obeys the Curie-Weiss law

$$\varepsilon' = \frac{C_{CW}}{T - \theta}, \tag{2}$$

where C_{CW} and θ are the Curie-Weiss constant and the Curie-Weiss temperature, respectively. In this case, the dependence of $1/\varepsilon'$ versus temperature (or temperature difference (T - θ)) should be linear.

The experimental $1/\varepsilon'(T)$ curves for both $0.5(Y_{0.1}Zr_{0.9}O_2)$ - $(0.6SrTiO_3$ – $0.4BiScO_3)$ and $0.6SrTiO_3$ – $0.4BiScO_3$ are really linear above some temperature T^* (Fig. 5(a)) Just below T^*, these curves start to deviate from the Curie-Weiss behavior.

In turn, the $\varepsilon'(T)$ dependence between the temperatures T^* and T_m can be fitted by expression [35]

$$\frac{\varepsilon'_m}{\varepsilon'(T)} = 1 + \frac{(T - T_m)^\gamma}{2S^2}, \tag{3}$$

where ε'_m is a maximum value of the dielectric permittivity, S is a degree of diffuseness of the phase transition and γ is a degree of the dielectric relaxation. For ferroelectrics with the sharp phase transition γ = 1 and a consistent diffusing the phase transition results in increasing γ up to 2. That is, larger values of γ express more relaxor behavior of the ferroelectric.

The dependences of $\ln[(\varepsilon'_m - \varepsilon'(T))/\varepsilon'(T)]$ versus $\ln(T - T_m)$ for the $0.5(Y_{0.1}Zr_{0.9}O_2)$ - $(0.6SrTiO_3$ – $0.4BiScO_3)$ and $0.6SrTiO_3$ – $0.4BiScO_3$ systems are shown in Fig. 5(b). One can see that expression (3) reproduces experimental data very well.

The T_m, ε'_m, C_{CW}, T^*, S and γ values for ternary $0.5(Y_{0.1}Zr_{0.9}O_2)$ - $(0.6SrTiO_3$ – $0.4BiScO_3)$ and two-component $0.6SrTiO_3$ – $0.4BiScO_3$ systems are listed in Table 3. One can see that the diffuse phase transition for ternary $0.5(Y_{0.1}Zr_{0.9}O_2)$ – $0.5(0.6SrTiO_3$ – $0.4BiScO_3)$ system is, firstly, the transition with less degree of the diffuseness and, secondly, it is positioned at lower temperatures as compared to two-component $0.6SrTiO_3$ – $0.4BiScO_3$ system. To account for this

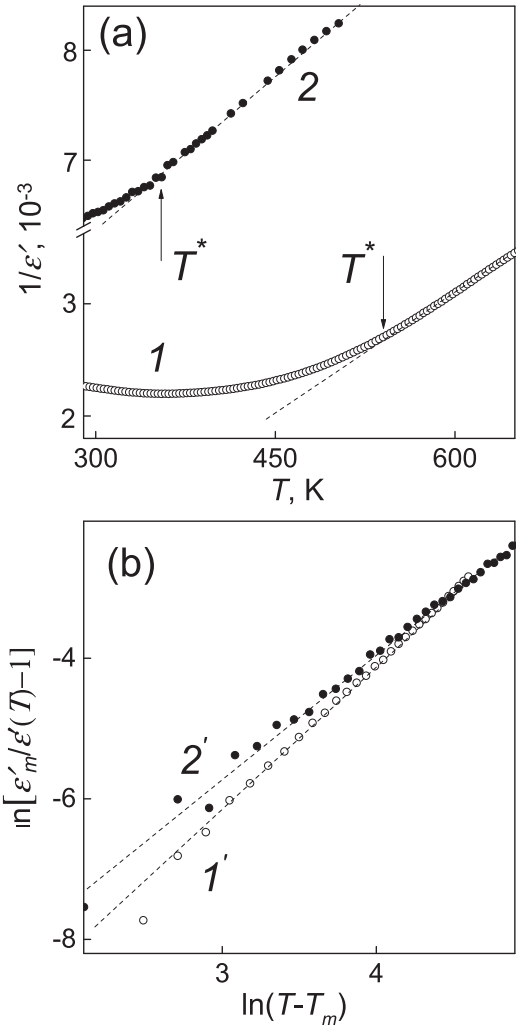

Fig. 5. The $1/\varepsilon'$ vs. T (a) and $\ln[(\varepsilon'_m - \varepsilon'(T))/\varepsilon'(T)]$ vs. $\ln(T - T_m)$ (b) dependences for the $0.5(Y_{0.1}Zr_{0.9}O_2)$ - $(0.6SrTiO_3 - 0.4BiScO_3$ (curves *1* and *1′*) and $0.6SrTiO_3 - 0.4BiScO_3$ (*2* and *2′*) systems.

Table 3
Parameters of the diffuse phase transition for ternary $0.5(Y_{0.1}Zr_{0.9}O_2) - 0.5(0.6SrTiO_3 - 0.4BiScO_3)$ and two-component $(1-x)SrTiO_3 - xBiScO_3$ systems.

Composition	T_m, K	ε'_m	C_{CW}, K	T^*, K	S, K	γ
$0.5(Y_{0.1}Zr_{0.9}O_2) - 0.5(0.6SrTiO_3 - 0.4BiScO_3)$	225	160	$9.3\cdot10^4$	385	105	1.75
$0.6SrTiO_3 - 0.4BiScO_3$	355	455	$13.2\cdot10^4$	540	305	2.00
$0.7SrTiO_3 - 0.3BiScO_3$	312	180	$10.4\cdot10^4$	505	149	1.71
$0.8SrTiO_3 - 0.2BiScO_3$	100	167	$6.8\cdot10^4$	320	105	1.58

peculiarity, it would be helpful to analyze an evolution of the diffuse phase transition in two-component $(1-x)SrTiO_3$-$xBiScO_3$ system with changing x. The parameters of the diffuse phase transition for this system corresponding to the compositions with $x = 0.2$ and 0.3 and reported earlier in Ref. [17] are also added to Table 3.

Analyzing the parameters of the diffuse phase transition in the $(1-x)SrTiO_3$-$xBiScO_3$ system for the compositions with $x = 0.2$, 0.3 and 0.4, it could be concluded that an increase x results in increase of the diffuseness degree, and shifts this phase transition to higher temperatures. As mentioned above, $SrTiO_3$ is an incipient ferroelectric lying near limit of its paraelectric phase stability and retaining their nonpolar centrosymmetric structure upon cooling at $T \rightarrow 0$ K. However, various impurities substituting for the host ions in *A*- or/and *B*-positions in the perovskite ABO_3 structure can induce a ferroelectric phase transition in $SrTiO_3$. Obviously, for two-component $(1-x)SrTiO_3$-$xBiScO_3$ system, the Bi ions substituting for Sr and the Sc ions substituting for Ti will distort the crystal $SrTiO_3$ structure resulting in an appearance of the diffuse ferroelectric phase transition at some temperature which depend on composition. Also obviously, that strength of this structure distortion will in turn be dependent on a difference in the ionic radii of the host and impurity ions. For the host ions these radii are equal to $r(Sr^{2+}) = 1.44$ Å and $r(Ti^{4+}) = 0.605$ Å, while Sc^{3+} and Bi^{3+} acting in this case as the impurity ions are characterized by $r(Sc^{3+}) = 0.745$ Å and $r(Bi^{3+}) = 1.03$ Å. Since for ternary $0.5(Y_{0.1}Zr_{0.9}O_2) - 0.5(0.6SrTiO_3 - 0.4BiScO_3)$ system the smaller Zr^{4+} ion partially substitutes for bigger Sc^{3+} ion in the $0.6SrTiO_3 - 0.4BiScO_3$ subsystem (Table 2), the crystal structure distortion of this subsystem should decrease as compared to that in two-component $0.6SrTiO_3 - 0.4BiScO_3$ system, as found experimentally (Table 3). Hence, the parameters of the diffuse phase transition for ternary $0.5(Y_{0.1}Zr_{0.9}O_2) - 0.5(0.6SrTiO_3 - 0.4BiScO_3)$ system does not coincide with the values for the composition with $x = 0.4$ for two-component $(1-x)SrTiO_3$-$xBiScO_3$ system and are better corresponded to the parameters lying between the values for the compositions with $x = 0.2$ and 0.3. Moreover, difference in valence of Sc^{3+} and Zr^{4+} is also seemed to influence on the diffuse phase transition in ternary $0.5(Y_{0.1}Zr_{0.9}O_2) - 0.5(0.6SrTiO_3 - 0.4BiScO_3)$ system. However, this issue will be not discussed here.

3.3. Dielectric properties peculiarities due to relaxation process

The dielectric anomalies of the second type for ternary $0.5(Y_{0.1}Zr_{0.9}O_2) - 0.5(0.6SrTiO_3 - 0.4BiScO_3)$ and two-component $0.6SrTiO_3 - 0.4BiScO_3$ systems are shown in Fig. 6. The temperature ε' and ε'' dependences presented in this figure were measured at frequency $\nu = 1$ kHz The dielectric anomalies lying in the temperature 500–800 K interval are observed as the step-like changes in the $\varepsilon'(T)$ dependences to whom the maxima in the $\varepsilon''(T)$ dependences correspond. It should be noted that the $\varepsilon'(T)$ and $\varepsilon''(T)$ changes are more pronounced for two-component system as compared to ternary system.

It was found that the temperature position of the $\varepsilon'(T)$ and $\varepsilon''(T)$ changes observed in Fig. 6 is dependent on measuring frequency. For instance, the $\varepsilon'(T)$ and $tg\delta(T)$ dependences for ternary $0.5(Y_{0.1}Zr_{0.9}O_2) - 0.5(0.6SrTiO_3 - 0.4BiScO_3)$ system taken at measuring frequencies of 600 Hz, 1 kHz, 4 kHz, 12 kHz and 45 kHz are shown in Fig. 7. It should be noted that besides ε'', the tangent of dielectric losses, $tg\delta$, is another quantity characterizing the dielectric properties of solids. A relation between ε'' and $tg\delta$ is expressed by $\varepsilon'' = \varepsilon' \cdot tg\delta$.

One can see that both step-like changes in the $\varepsilon'(T)$ dependence and maximum in the $tg\delta(T)$ dependences are shifted to higher temperatures with increasing measuring frequency. Such kind of behavior is characteristic for dielectric relaxation processes [8–10,36–38].

The dielectric relaxation process is characterized by a relaxation time, τ. Two ways can be used to estimate τ. According to the first way, the τ value taken as $\tau = 1/2\pi\nu$ for determined measuring frequency is corresponding to the temperature at which the $tg\delta(T)$ maximum occurs, that allows recovering the $\tau(T)$ dependence using the $tg\delta(T)$ curves measured at various frequencies. In the framework of the second way, so-called Cole-Cole plots should be plotted to extract τ. The Cole-Cole plots are the $\varepsilon'' = f(\varepsilon')$ dependences, where each pair of the ε'' and ε' values corresponds to determined measuring frequency. In turn, to obtain these plots, the frequency dependences of ε' and ε'' have to be measured at various temperatures.

We applied both ways to estimate τ for ternary $0.5(Y_{0.1}Zr_{0.9}O_2) - (0.6SrTiO_3 - 0.4BiScO_3)$ system and two-component $0.6SrTiO_3 - 0.4BiScO_3$ system. The τ estimates happened to be very close each to other for both ways. So, further it would be reasonably used one way to estimate τ for one system studied, and to apply other way to estimate τ for other system.

The first way was used to extract τ for ternary $0.5(Y_{0.1}Zr_{0.9}O_2) -$

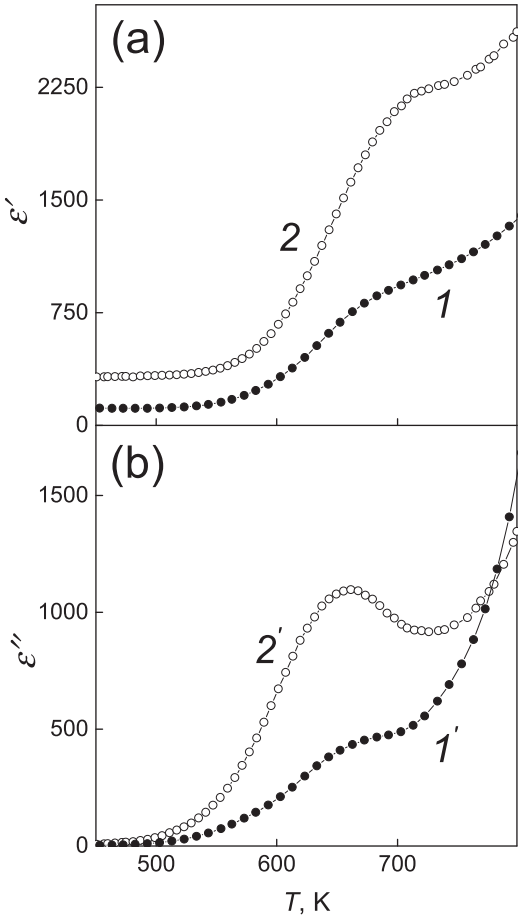

Fig. 6. The temperature ε' (a) and ε'' (b) dependences for the $0.5(Y_{0.1}Zr_{0.9}O_2)$ - $(0.6SrTiO_3 – 0.4BiScO_3)$ (curves *1* and *1′*) and $0.6SrTiO_3 – 0.4BiScO_3$ (*2* and *2′*) systems for the dielectric relaxation.

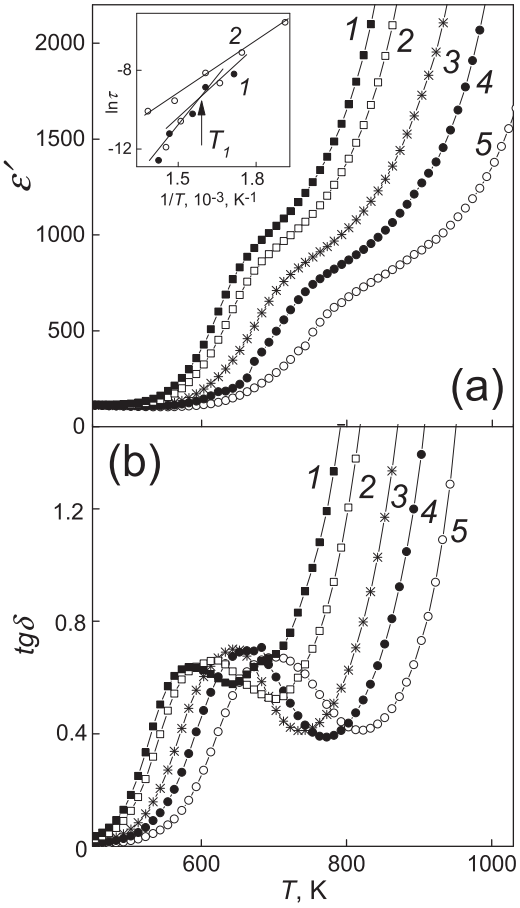

Fig. 7. The temperature ε' (a) and $tg\delta$ (b) dependences for the $0.5(Y_{0.1}Zr_{0.9}O_2)$ - $(0.6SrTiO_3 – 0.4BiScO_3)$ system taken at frequencies of 600 Hz (curve *1*), 1 kHz (*2*), 4 kHz (*3*), 12 kHz (*4*) and 45 kHz (*5*). Inset to Fig. (a): the $\ln\tau$ vs. $1/T$ dependences for the $0.5(Y_{0.1}Zr_{0.9}O_2)$ - $(0.6SrTiO_3 – 0.4BiScO_3)$ system (curve *1*) and the $0.6SrTiO_3 – 0.4BiScO_3$ system (*2*).

$(0.6SrTiO_3 – 0.4BiScO_3)$ system. It was found that τ rapidly decreases with increasing temperature from $\sim 2.74\cdot10^{-4}$ s at ~ 583 K (it is the temperature of the $tg\delta(T)$ maximum at 600 Hz) down to $\sim 3.46\cdot10^{-6}$ s at ~ 702 K (it is the temperature of the $tg\delta(T)$ maximum at 45 kHz). Next it was tested, whether the $\tau(T)$ dependence can be described by the Arrhenius law, which can be expressed as

$$\tau = \tau_0 \exp(E_D/k_B T), \quad (4)$$

where τ_0 is the inverse of attempt frequency, E_D is the activation energy of the dielectric relaxation process and k_B is the Boltzmann constant.

The $\ln\tau$ versus $1/T$ dependence for ternary $0.5(Y_{0.1}Zr_{0.9}O_2)$ - $(0.6SrTiO_3 – 0.4BiScO_3)$ system is presented in the inset to Fig. 7(a). The $tg\delta(T)$ dependences measured at frequencies of 200 Hz, 900 Hz, 6.3 kHz and 23 kHz were additionally used to obtain the reliable $\ln\tau$ versus $1/T$ dependence. This dependence can be considered as consisting of two parts intersecting at some temperature $T_1 \approx 600$ K. A slope of the lines for two parts allows estimating the activation energy as $E_{D1} \approx 0.9$ eV at $T > T_1$ and $E_{D1} \approx 1.3$ eV at $T < T_1$.

In contrast to ternary system, the Cole-Cole plots were used to extract τ for two-component $0.6SrTiO_3 – 0.4BiScO_3$ system. To do so, the frequency dependences of ε' and ε'' taken for various temperatures were preliminary measured (Fig. 8). One can see that both ε' and ε'' rapidly fall with increasing frequency that is also characteristic for dielectric relaxation process. Next, the $\varepsilon'(\nu)$ and $\varepsilon''(\nu)$ dependences were used to plot the $\varepsilon'' = f(\varepsilon')$ dependences as the Cole-Cole plots at various temperatures (Fig. 9). One can see that the data points fit well into semicircular arcs. The centers of the arcs are positioned underneath the abscissa that can be related to some deviation of the dielectric relaxation observed in the $0.6SrTiO_3 – 0.4BiScO_3$ system from the ideal Debye model usually used to describe dielectric relaxation processes in solids. In this case, the complex dielectric permittivity, $\varepsilon^* = \varepsilon' - i\varepsilon''$, can empirically be described by the Cole-Cole equation [8]

$$\varepsilon^* = \varepsilon_\infty + \frac{(\varepsilon_0 - \varepsilon_\infty)}{1+(i\omega\tau)^{1-\alpha}}, \quad (5)$$

where ε_o is the static dielectric permittivity, ε_∞ is the permittivity at high frequency, ω is the angular frequency, and α is the angle of the semicircular arc.

By fitting the experimental data in Fig. 9 by Eq. (5), the relaxation time can be found for various temperatures. The $\tau(T)$ dependence was found to very well obey the Arrhenius law (expression (4)). The $\ln\tau$ versus $1/T$ dependence for two-component $0.6SrTiO_3 – 0.4BiScO_3$ system is also presented in the inset to Fig. 7(a). In contrast to ternary $0.5(Y_{0.1}Zr_{0.9}O_2)$ - $(0.6SrTiO_3 – 0.4BiScO_3)$ system, this dependence is corresponding to one linear part with the activation energy estimated as ~ 0.75 eV which is remarkably less than the E_D values for ternary $0.5(Y_{0.1}Zr_{0.9}O_2)$ - $(0.6SrTiO_3 – 0.4BiScO_3)$ system.

It should be also noted that linear parts observed in the Cole-Cole plots at high temperatures and low frequencies can be related to high electrical conductivity.

Now, let us discuss the peculiarities of the dielectric relaxation processes observed in ternary $0.5(Y_{0.1}Zr_{0.9}O_2)$ - $(0.6SrTiO_3 – 0.4BiScO_3)$ and two-component $0.6SrTiO_3 – 0.4BiScO_3$ systems. First of all, it should be noted that the dielectric relaxation process like found in the systems studied can occur in both $Y_{0.1}Zr_{0.9}O_2$ subsystem [39] and

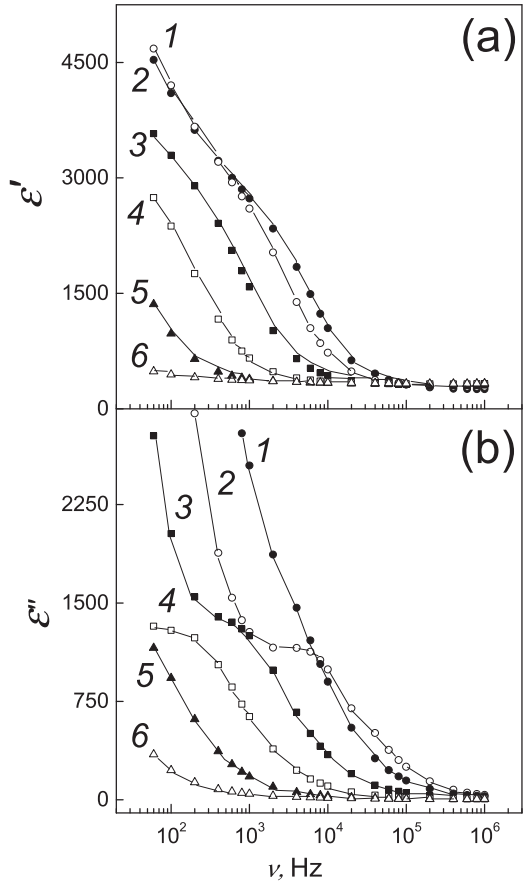

Fig. 8. The frequency ε' (a) and ε'' (b) dependences for the $0.6SrTiO_3$ – $0.4BiScO_3$ system taken at temperatures of 723 (curve *1*), 673 (*2*), 623 (*3*), 573 (*4*), 523 (*5*) and 473 K (*6*).

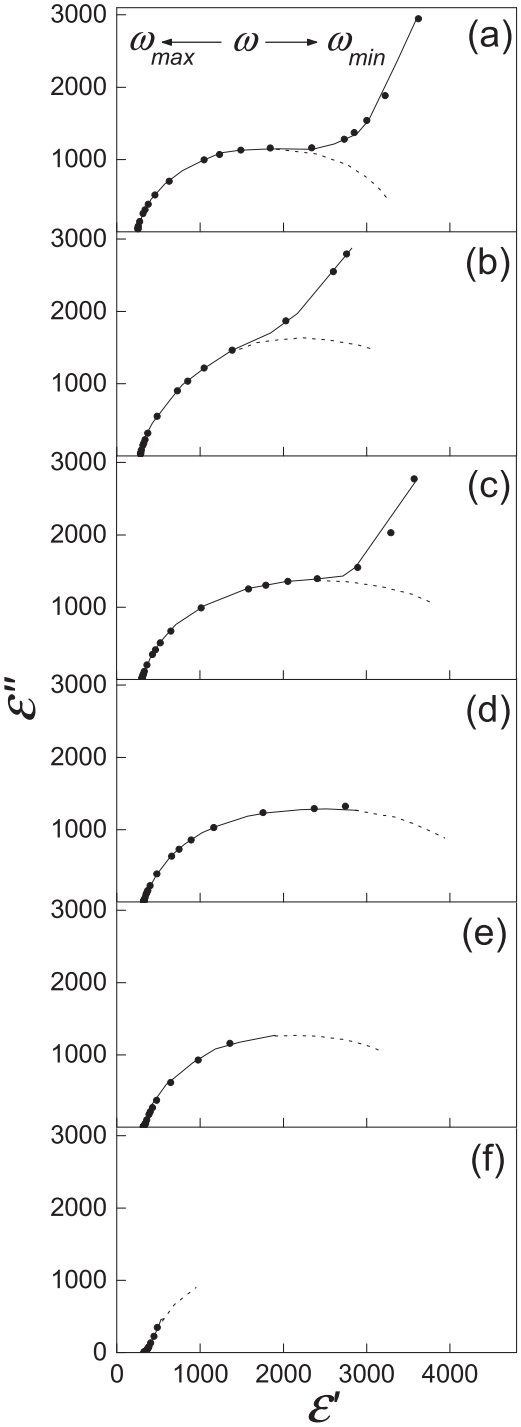

Fig. 9. The Cole-Cole plots for the $0.6SrTiO_3$ – $0.4BiScO_3$ system plotted for temperatures of 723 (a), 673 (b), 623 (c), 573 (d), 523 (e) and 473 K (f).

$SrTiO_3$ – $BiScO_3$ subsystem [36–38]. The dielectric relaxation in both subsystems is often attributed to oxygen vacancy hoppings related to the O^{2-} ions migration. The migration energy corresponding to the activation energy of the dielectric relaxation process can be related to potential barriers which have to be overcome by the O^{2-} ions during their migration in the electric field direction. For two-component $0.6SrTiO_3$ – $0.4BiScO_3$ system one dielectric relaxation process with $E_D \approx 0.75$ eV takes place, since one linear part was observed in the $\ln\tau$ versus $1/T$ dependence. However, two dielectric relaxation processes having the different E_D values were found in ternary $0.5(Y_{0.1}Zr_{0.9}O_2)$ - $(0.6SrTiO_3 – 0.4BiScO_3)$ system. Taking into account the estimated E_D values, the relaxation process with $E_{D1} \approx 0.9$ eV could be believed to be related to the $SrTiO_3$ – $BiScO_3$ subsystem, whereas the $Y_{0.1}Zr_{0.9}O_2$ subsystem is responsible for the dielectric relaxation process with $E_{D1} \approx 1.3$ eV. If E_D and E_{D1} are corresponding to the dielectric relaxation processes in two-component $0.6SrTiO_3$ – $0.4BiScO_3$ system or in the $SrTiO_3$ – $BiScO_3$ subsystem in ternary $0.5(Y_{0.1}Zr_{0.9}O_2)$ - $(0.6SrTiO_3 – 0.4BiScO_3)$ system, respectively, then the difference between E_D and E_{D1} could be originated from a change of the composition of these systems during the synthesis (Table 2). It is known [40] that the height of the potential barriers overcame by migrating O^{2-} ions is dependent on presence and content of the impurity. It would be helpful to compare the E_D values estimated for the samples studied with the activation energy known from literature data for similar ceramic systems demonstrating the high-temperature dielectric relaxation processes due to the oxygen vacancy hoppings. These activation energies were earlier reported as equal to 0.99 eV for $Sr_{0.8}Bi_{0.133}TiO_3$ [8], 1.57 eV for $Pb_{0.9}La_{0.1}TiO_3$ and 1.8 eV for $Pb_{0.8}La_{0.2}TiO_3$ [36], 1.03 eV for $Ce_{0.8}Y_{0.2}O_{1.9}$ [39], 1.18 eV for $0.5(BiFeO_3)$ – $0.5((KBi)_{1/2}TiO_3)$ [41], 1.3 eV for $0.8((KBi)_{1/2}TiO_3)$ – $0.2Na_{1/4}Bi_{3/4}Fe_{1/2}Ti_{1/2}O_3$ [42], 0.48 eV for $(Pb_{1-x}La_x)(Zr_{0.90}Ti_{0.10})_{1-x/4}O_3$ with $x = 0.2$ [43], 0.42–0.575 eV for $(Bi_{0.90}R_{0.10})Fe_{0.95}Sc_{0.05}O_3$ [R = La, Nd] [44]. So, the E_D values extracted for ternary $0.5(Y_{0.1}Zr_{0.9}O_2)$ – $0.5(0.6SrTiO_3 – 0.4BiScO_3)$ system and two-component $0.6SrTiO_3$ – $0.4BiScO_3$ system are in agreement with the activation energy estimates obtained for other similar ceramics systems.

It should be noted the O^{2-} ions migration, on the one hand, will form a dipole moment resulting in the dielectric relaxation process discussed above. On the other hand, the diffusion of oxygen ions via oxygen vacancies is the main electrical conduction process at high temperatures

in both ZrO_2 and perovskite compounds. However, the activation energy for the dielectric relaxation process is corresponding to only the migration energy associated with the jump of an O^{2-} ion, which requires ionic displacement around a saddle point in a diffusion path [39]. Besides the migration energy, the dissociation energy of an oxygen vacancy from the restrained state will additionally contribute to the total activation energy for oxygen ionic conductivity.

At present, research of oxygen ionic conductivity in ternary $0.5(Y_{0.1}Zr_{0.9}O_2)$ - $(0.6SrTiO_3 – 0.4BiScO_3)$ system are in progress. Results of this research will be published elsewhere.

4. Conclusion

The ceramic samples of ternary $0.5(Y_{0.1}Zr_{0.9}O_2) – 0.5(0.6SrTiO_3 – 0.4BiScO_3)$ system consisting of the individual $Y_{0.1}Zr_{0.9}O_2$ and $0.6SrTiO_3 – 0.4BiScO_3$ subsystems were prepared via solid-state processing techniques. The tetragonal *P42/nmc* phase related to the $Y_{0.1}Zr_{0.9}O_2$ subsystem and, the cubic $Pm\bar{3}m$ and tetragonal *P4mm* phases attributed to the $0.6SrTiO_3 – 0.4BiScO_3$ subsystem were found to coexist at room temperature. A deviation of real composition from nominal one for both $Y_{0.1}Zr_{0.9}O_2$ and $0.6SrTiO_3 – 0.4BiScO_3$ subsystems was observed. This deviation is mainly due to Sc substituting for Zr in the $Y_{0.1}Zr_{0.9}O_2$ subsystem and, vice versa, Zr substituting for Sc in the $SrTiO_3 – BiScO_3$ subsystem.

The dielectric properties peculiarities due to both diffuse phase transition and dielectric relaxation processes observed in ternary system were compared to these peculiarities earlier reported for two-component $0.6SrTiO_3 – 0.4BiScO_3$ system. The composition change of the $0.6SrTiO_3 – 0.4BiScO_3$ subsystem in ternary system results in a degree decrease of the transition diffuseness, and shifts the transition to lower temperatures as compared to two-component system. These tendencies could be related to a difference of ionic radii of Zr^{4+} and Sc^{3+} ions.

The step-like changes in the $\varepsilon'(T)$ dependences and the maxima in the $\varepsilon''(T)$ dependences observed in both ternary and two-component systems within the temperature 500–800 K interval are related to the dielectric relaxation processes. This processes associated with the O^{2-} ions migration creating a dipole moment can occur in both systems. Two dielectric relaxation processes related to the $Y_{0.1}Zr_{0.9}O_2$ and $0.6SrTiO_3 – 0.4BiScO_3$ subsystems were found in ternary system, whereas one dielectric relaxation process was observed in two-component system.

Acknowledgements

O. I. thanks the Ministry of Education and Science of the Russian Federation for the financial support under project No 3.6586.2017/6.7. All of studies were carried out by the scientific equipment of joint research center "Technologies and Materials" at the Belgorod State University.

Declarations of interest

None.

References

[1] S. Tao, J.T.S. Irvine, Optimization of mixed conducting properties of Y_2O_3-ZrO_2-TiO_2 and Sc_2O_3-Y_2O_3-ZrO_2-TiO_2 solid solutions as potential SOFC anode materials, J. Solid State Chem. 165 (2002) 12–18.
[2] M. Nakatou, N. Miura, Impedance metric sensor based on YSZ and In_2O_3 for detection of low concentrations of water vapor at high temperature, Electrochem. Commun. 6 (2004) 995–998.
[3] C.O. Park, S.A. Akbar, W. Weppner, Ceramic electrolytes and electrochemical sensors, J. Mater. Sci. 38 (2003) 4639–4660.
[4] J.G. Duh, H.T. Dai, B.S. Chiou, Sintering, microstructure, hardness, and fracture toughness behavior of Y_2O_3–CeO_2–ZrO_2, J. Am. Ceram. Soc. 71 (1988) 813–819.
[5] Y. Zhang, J. Malzbender, D.E. Mack, M.O. Jarligo, X. Cao, Q. Li, R. Vaßen, D. Stöver, Mechanical properties of zirconia composite ceramics, Ceram. Int. 39 (2013) 7595–7603.
[6] K.A. Muller, H. Burkard, $SrTiO_3$: an intrinsic quantum paraelectric below 4 K, Phys. Rev. B 9 (1979) 3593–3602.
[7] V.V. Lemanov, Improper ferroelastic $SrTiO_3$ and what we know today about its properties, Ferroelectrics 265 (2002) 1–21.
[8] C. Ang, Z. Yu, L.E. Cross, Oxygen-vacancy-related low-frequency dielectric relaxation and electrical conduction in Bi: $srtio_3$, Phys. Rev. B 62 (2000) 228–236.
[9] C. Ang, Z. Yu, P. Lunkenheimer, J. Hemberger, A. Loidl, Dielectric relaxation modes in bismuth-doped $SrTiO_3$: the relaxor behavior, Phys. Rev. B 59 (1999) 6670–6674.
[10] V.V. Lemanov, E.P. Smirnova, A.V. Sotnikov, M. Weihnacht, Dielectric relaxation in $SrTiO_3$-$SrMg_{1/3}Nb_{2/3}O_3$ and $SrTiO_3$-$SrSc_{1/3}Ta_{2/3}O_3$ solid solutions, Appl. Phys. Lett. 77 (2000) 4205–4207.
[11] C. Ang, Z. Yu, P.M. Vilarinho, J.P. Baptista, Bi: $srtio_3$: a quantum ferroelectric and a relaxor, Phys. Rev. B 57 (1998) 7403–7406.
[12] J.G. Bednorz, K.A. Muller, $Sr_{1-x}Ca_xTiO_3$: an XY quantum ferroelectric with transition to randomness, Phys. Rev. Lett. 52 (1984) 2289–2301.
[13] R.E. Eitel, C.A. Randall, T.R. Shrout, S.E. Park, Preparation and characterization of high temperature perovskite ferroelectrics in the solid-solution $(1 – x)BiScO_3 – xPbTiO_3$, Jpn. J. Appl. Phys. 41 (2002) 2099–2104.
[14] S. Zhang, C.A. Randall, T.R. Shrout, High Curie temperature piezocrystals in the $BiScO_3 – PbTiO_3$ perovskite system, Appl. Phys. Lett. 83 (2003) 3150–3152.
[15] H. Ogihara, C.A. Randall, S. Trolier-McKinstry, Weakly coupled relaxor behavior of $BaTiO_3$–$BiScO_3$ ceramics, J. Am. Ceram. Soc. 92 (2009) 110–118.
[16] S. Trolier-McKinstry, M.D. Biegalski, J. Wang, A.A. Belik, E. Takayama-Muromach, I. Levin, Growth, crystal structure, and properties of epitaxial $BiScO_3$ thin films, J. Appl. Phys. 104 (2008) (044102-01-07).
[17] O. Ivanov, E. Danshina, Y. Tuchina, V. Sirota, Ferroelectricity in $SrTiO_3 – BiScO_3$ system, Phys. Status Solidi B 248 (2011) 1006–1009.
[18] O. Ivanov, E. Danshina, Y. Tuchina, V. Sirota, Diffuse phase transition and ferroelectric properties of ceramic solid solution in new $SrTiO_3$ - $BiScO_3$ system, Adv. Sci. Technol. 67 (2010) 59–63.
[19] L.E. Cross, Relaxor ferroelectrics, Ferroelectrics 151 (1994) 305–320.
[20] K. Hirota, Z.G. Ye, S. Wakimoto, P.M. Gehring, G. Shirane, Neutron diffuse scattering from polar nanoregions in the relaxor $Pb(Mg_{1/3}Nb_{2/3})O_3$, Phys. Rev. B 65 (2002) 104–1055.
[21] S.A. Gridnev, Dielectric relaxation in disordered polar dielectrics, Ferroelectrics 266 (2002) 171–209.
[22] K. Tsuzuku, S. Taruta, N. Takusagawa, H. Kishi, Dielectric properties of sintered materials prepared glass-ZrO_2-$SrTiO_3$ mixtures, J. Mater. Sci. Mater. Electron. 11 (2000) 419–424.
[23] J. Garcia-Barriocanal, A. Rivera-Calzada, M. Varela, Z. Sefrioui, M.R. Diaz-Guillen, K.J. Moreno, J.A. Diaz-Guillen, E. Iborra, A.F. Fuentes, S.J. Pennycook, C. Leon, J. Santamaria, Tailoring disorder and dimensionality: strategies for improved solid oxide fuel cell electrolytes, ChemPhysChem 10 (2009) 1003–1011.
[24] J. Garsia-Barriocanal, A. Rivera-Calzada, M. Varela, Z. Sefrioui, M.R. Diaz-Guillen, K.J. Moreno, J.A. Diaz-Guillen, E. Iborra, A.F. Fuentes, S.J. Pennycook, C.J. Santamaria, Colossal ionic conductivity at interfaces of epitaxial ZrO_2:Y_2O_3/$SrTiO_3$ heterostructures, ChemPhysChem 10 (2009) 676–680.
[25] T. Pennycook, M.P. Oxley, Seeing oxygen disorder in YSZ/$SrTiO_3$ colossal ionic conductor heterostructures using EELS, Eur. Phys. J. Appl. Phys. 54 (2011) 3507–3511.
[26] A. Diaz-Guillen, M.R. Diaz-Guillen, K.P. Padmasree, A.F. Fuentes, J. Santamaria, C. Leon, Effect of La substitution for Gd in the ionic conductivity and oxygen dynamics for fluorite-type $Gd_2Zr_2O_7$, Solid State Ion. 179 (2008) 2160–2164.
[27] O.N. Ivanov, E.P. Danshina, D.A. Kolesnikov, Coexistence of the cubic and tetragonal phases in relaxor ferroelectric $SrTiO_3$-$BiScO_3$ system, Ferroelectrics 444 (2013) 130–136.
[28] A.A. Belik, S. Iikubo, K. Kodama, N. Igawa, S. Shamoto, M. Maie, T. Nagai, Y. Matsui, S.Y. Stefanovich, B.I. Lazoryak, E. Takayama-Muromachi, $BiScO_3$: centrosymmetric $BiMnO_3$-type oxide, J. Am. Chem. Soc. 128 (2006) 706–707.
[29] A. Savitzky, M.J.E. Golay, Smoothing and differentiation of data by simplified least squares procedures, Anal. Chem. 36 (1964) 1627–1639.
[30] E.J. Sonneveld, J.W. Visser, Automatic collection of powder data from photographs, J. Appl. Cryst. 8 (1975) 1–7.
[31] H. Toraya, Effect of $YO_{1.5}$ dopant on unit-cell parameters of ZrO_2 at low contents of $YO_{1.5}$, J. Am. Ceram. Soc. 72 (1989) 662–664.
[32] F.J. Humphreys, M. Hatherly, Recrystallization and Related Annealing Phenomena, Elsevier, Oxford, UK, 2004.
[33] V.V. Shvartsman, D.C. Lupascu, Lead free relaxor ferroelectrics, J. Am. Ceram. Soc. 95 (2012) 1–26.
[34] J. Toulouse, The three characteristic temperatures of relaxor dynamics and their meaning, Ferroelectrics 369 (2008) 203–213.
[35] C.-C. Huang, D.P. Cann, X. Tan, N. Vittayakorn, Phase transitions and ferroelectric properties in$BiScO_3 – Bi(Zn_{1/2}Ti_{1/2})O_3 – BaTiO_3$ solid solutions, J. Appl. Phys. 102 (2007) (044103-1-044103-5).
[36] B.S. Kang, S.K. Choi, C.H. Park, Diffuse dielectric anomaly in perovskite-type ferroelectric oxides in the temperature range of 400–700 °C, J. Appl. Phys. 94 (2003) 1904–1911.
[37] C. Ang, Z. Yu, J. Hemberger, P. Lunkenheimer, A. Loidl, Dielectric anomalies in bismuth-doped $SrTiO_3$: defect modes at low impurity concentrations, Phys. Rev. B 59 (1999) 6665–6669.
[38] D.W. Johnson, L.E. Cross, F.A. Hummel, Dielectric relaxation in strontium titanates containing rare-earth ions, J. Appl. Phys. 41 (1970) 2828–2833.
[39] K.P. Padmasree, R.A. Montalvo-Lozano, S.M. Montemayor, A.F. Fuentes, Electrical conduction and dielectric relaxation process in $Ce_{0.8}Y_{0.2}O_{1.9}$ electrolyte, J. Alloy.

Compd. 509 (2011) 8584–8589.
[40] V.G. Zavodinsky, The mechanism of ionic conductivity in stabilized cubic zirconia, Phys. Solid State 46 (2004) 453–457.
[41] A. Pushkarev, N. Olekhnovich, Yu Radyush, Dielectric properties of perovskite ceramics of $(1- x)BiFeO_3 - x(KBi)_{1/2}TiO_3$ ($0.40 < x < 0.85$) solid solutions from impedance spectroscopy data, Phys. Solid State 53 (2011) 522–526.
[42] N. Yu. Radyush, A. Olekhnovich, Pushkarev, Dielectric properties of solid solutions $(1 - x)(KBi)_{1/2}TiO_3$-$xNa_{1/4}Bi_{3/4}Fe_{1/2}Ti_{1/2}O_3$ near the morphotropic phase boundary, Phys. Solid State 53 (2012) 91–97.
[43] A. Peláiz-Barranco, J.D.S. Guerra, Dielectric relaxation related to single-ionized oxygen vacancies in $(Pb_{1-x}La_x)(Zr_{0.90}Ti_{0.10})_{1-x/4}O_3$ ceramics, Mater. Res. Bull. 45 (2010) 1311–1313.
[44] I. Coondoo, N. Panwar, M. Asif Rafiq, V.S. Puli, M.N. Rafiq, R.S. Katiyar, Structural, dielectric and impedance spectroscopy studies in $(Bi_{0.90}R_{0.10})Fe_{0.95}Sc_{0.05}O_3$ [R = La, Nd] ceramics, Ceram. Int. 40 (2014) 9895–9902.